Supporting Information

A New Layered Sodium Molybdenum Oxide Anode for Full Intercalation-Type Sodium-Ion Batteries

Kai Zhu,[ab] Shaohua Guo,[a*] Jin Yi,[a] Songyan Bai,[a] Yingjin Wei,[b*] Gang Chen[b] and Haoshen Zhou[a,c*]

a Energy Technology Research Institute, Institution National Institute of Advanced Industrial Science and Technology (AIST), Umezono 1-1-1, Tsukuba, Japan

b Key Laboratory of Physics and Technology for Advanced Batteries (Ministry of Education), College of Physics, Jilin University, Qianjin Street 2699, Changchun, China

c National Laboratory of Solid State Microstructures & Department of Energy Science, Nanjing University, Nanjing 210093, China

*Corresponding authors: *guo.shaohua@outlook.com*; *yjwei@jlu.edu.cn*; *hs.zhou@aist.go.jp*

Experimental

Synthesis

Layered $Na_{0.3}MoO_2$ sample was synthesized by a one-step solid-state reaction. A proportionable mixture of reagent grade Na_2CO_3 (20% excess) and MoO_2 was ball-milled under wet condition with alcohol additions for 20 h at 200 rpm. After drying at 80 °C for 12 h, the obtained powder was pressed into pellets. Finally, the pellets were heated at 750 °C for 15 h under an Ar atmosphere. The obtained material was stored in an argon-filled glove box.

Layered $Na_{0.8}Ni_{0.4}Ti_{0.6}O_2$ is prepared as our previous report. The precursors of Na_2CO_3, NiO and TiO_2 were also ball-milled under wet condition with alcohol additions for 20 h at 200 rpm. After drying 80 °C for 12 h, the mixture was pressed into pellets and heated at 900 °C for 20 h under an Ar flow. The as-prepared materials was also stored in an argon-filled glove box.

Characterization

The crystalline structure and *ex-situ* XRD was characterized by Bruker D8 Advance Diffractometer using Cu Ka radiation. The morphology of as-prepared materials was observed using scanning electron microscopy (SEM, TOPCON DS-720 instrument). Transmission electron microscope (TEM) and high-resolution transmission electron microscope (HRTEM) were performed on a FEI Tacnai G2 electron microscope equipped with an X-ray energy dispersive spectroscopy (EDS, BRUKER AXS).

Electrochemical test

The electrochemical experiments were performed using 2032-type coin cells, with sodium metal served as the counter electrode, which were assembled in an argon-filled glove box. The working electrode was prepared by mixing 70 wt% of active material, 20 wt% of carbon black conductive additive and 10 wt% of poly-vinylidenefluoride (PVDF) binder onto aluminium foil. Mass loading of the electrode is about 2.5~3 mg/cm^2. The working and counter electrodes were separated by glass fiber membrane. The electrolyte was 1 M $NaPF_6$ in ethylene carbonate–diethyl carbonate (EC/DEC, 1 : 1 (v/v)). Galvonostatic charge – discharge was performed on a Hokuto Denko HJ1001SD8 battery tester in the voltage window of 0.05 – 2.0 V. Cyclic voltammetry (CV) was performed on Solartron 1640. For the full cell, the pre-desodiation of $Na_{0.8}Ni_{0.4}Ti_{0.6}O_2$ and pre-sodiation of $Na_{0.3}MoO_2$ were performed to carry out the three cycles' activation. $Na_{0.8}Ni_{0.4}Ti_{0.6}O_2$ /Na half cells were cycled in

the voltage range of 1.5-4 V at current density of 20 mA/g to get the pre-desodiation of $Na_{0.8}Ni_{0.4}Ti_{0.6}O_2$. And $Na_{0.3}MoO_2$/Na half cells were cycled in the voltage range of 0.05-2 V at current density of 20 mA/g to get pre-sodiation of $Na_{0.3}MoO_2$. The electrode mass ration of cathode and anode is around 1.2. The full cell is cathode limited and cycled in the voltage of 0.6-3.6 V.

Table S1 The sodium storage properties for reported titanium-based materials.

	Current density	Voltage range	Capacity	Cycle number	Capacity retention
$Na_2Ti_6O_{13}$[1]	5 mA/g	0-2.5 V	200 mAh/g	30	40%
$Na_2Ti_3O_7$[2]	17.7 mA/g	0.01-2.5 V	135 mAh/g	25	50%
$Na_4Ti_5O_{12}$[3]	12.5 mA/g	0.1-2.5 V	70 mAh/g	50	80%
$Na_{2/3}Co_{1/3}Ti_{2/3}O_2$[4]	20 mA/g	0.15-2.5 V	90 mAh/g	-	-
$Na_{2/3}Ni_{1/3}Ti_{2/3}O_2$[5]	22.5 mA/g	0.2-2 V	75 mAh/g	22	60%
$Na_{0.3}MoO_2$ (this work)	**20 mA/g**	**0.05-2 V**	**140 mAh/g**	50	**85%**

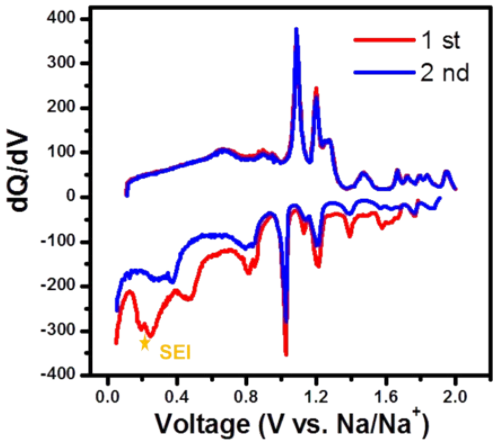

Figure S1 The dQ/dV curves of the $Na_{0.3}MoO_2$ at current density of 20 mA/g.

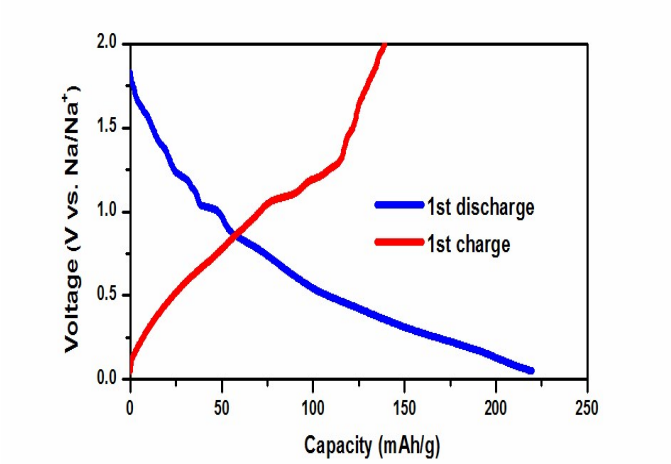

Figure S2 Disharge-charge curves of the $Na_{0.3}MoO_2$ for the first cycle at current density of 20 mA/g.

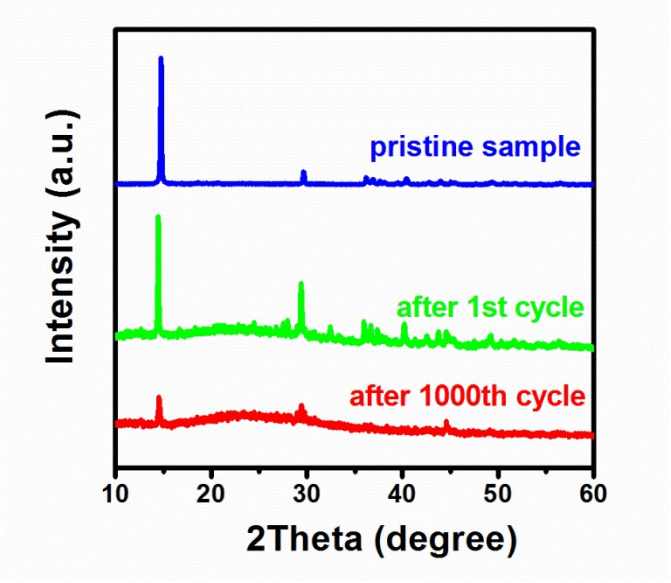

Figure S3 Standard XRD pattern of $Na_{0.3}MoO_2$ and *ex-situ* XRD patterns of $Na_{0.3}MoO_2$ after first and 1000th cycles.

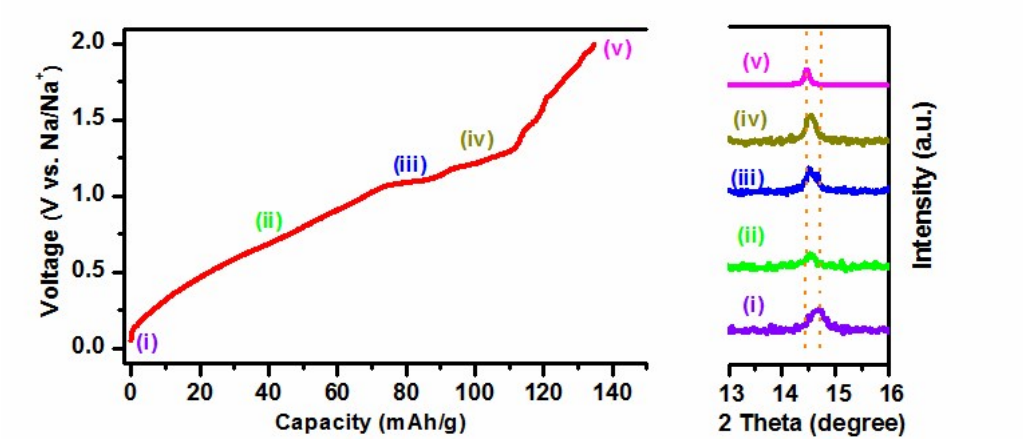

Figure S4 *Ex-situ* XRD patterns at different charge depths of the first cycle

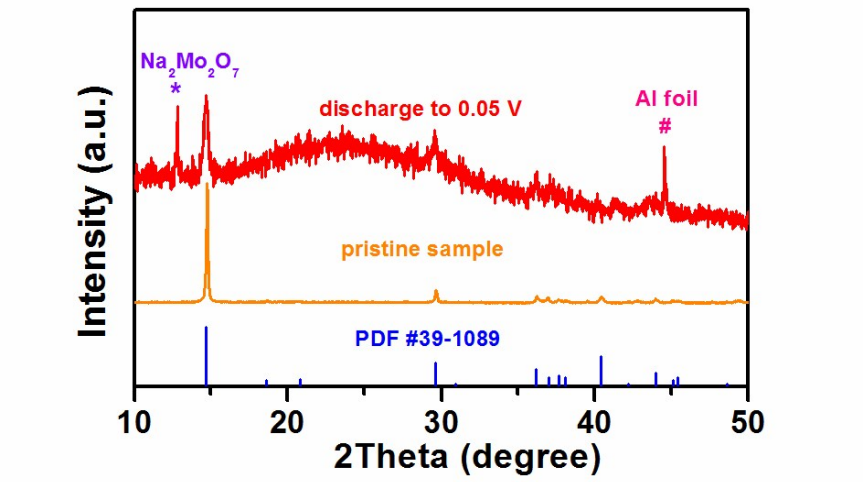

Figure S5 *Ex-situ* XRD pattern of $Na_{0.3}MoO_2$ after first discharge process.

$Na_{0.3}MoO_2$ as anode is a typical intercalation-type material based on following reasons:

1, From dQ/dV curves (as shown in **Figure S1**), it is clear that the position of the peaks do not change between the 1st and 2nd cycles, while for the alloying or conversion reaction, there are obvious change of the peaks position and peak intensity. [6-9] It would be characterized by the typical intercalation reaction.[10-12]

2, The reversible capacity is about 146 mAh/g, corresponding to 0.7 reversible sodium ion (de)intercalation in per $Na_{0.3}MoO_2$. The amount of sodium ions suggests that the sodium ion insertion into the $Na_{0.3}MoO_2$ to form $NaMoO_2$ as the following equation:

$$Na_{0.3}MoO_2 + 0.7Na^+ + 0.7e^- \rightarrow NaMoO_2$$

For the alloying or conversion reaction, more sodium ions will react with the electrode materials.[9-12]

3, The *ex-situ* XRD patterns at different charge depths of the first cycle (as shown in the right of **Figure S4**) display a shift of peak position during the sodium ion insertion into the anode materials. It is a typical phenomenon for the intercalation-type anode. [13, 14] Due to the low valence state of Mo is sensitive to the O_2, some impurity such as $Na_2Mo_2O_7$ are formed during the XRD testing in the air environment.

4, From the *ex-situ* XRD patterns after the 1st discharge as shown in **Figure S5**, it shows that peaks of $Na_{0.3+x}MoO_2$ are obvious and no peaks belonging to Mo metal or NaMo alloys are detected. It suggests that the $Na_{0.3}MoO_2$ is a typical intercalation-type anode. [15, 16]

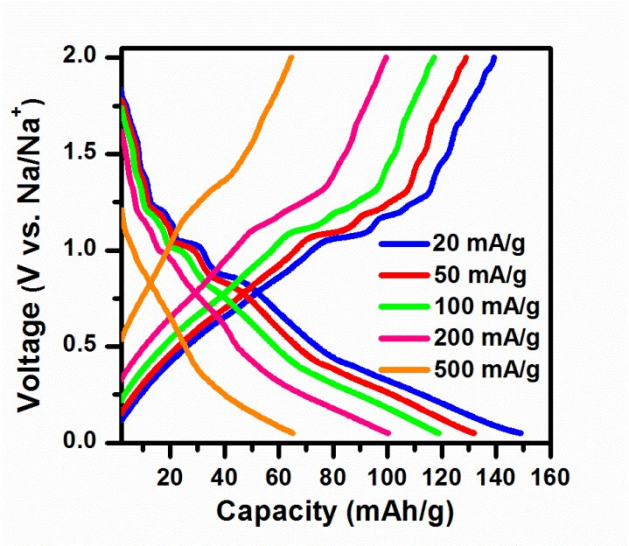

Figure S6 Discharge-charge profiles of the sample at different current densities.

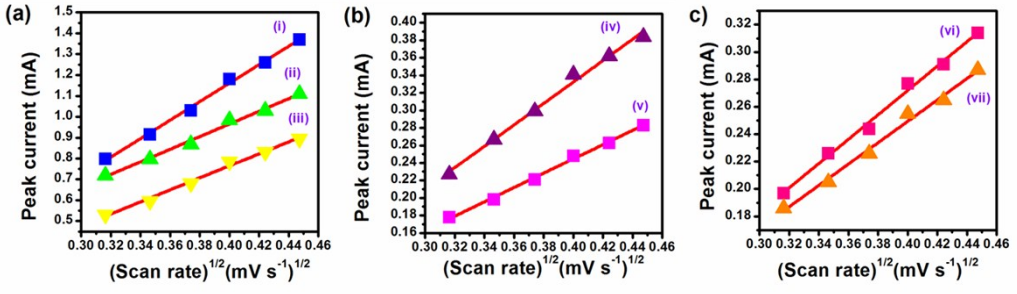

Figure S7 Linear fitting of I_p vs. $v^{1/2}$ relationship of the sample.

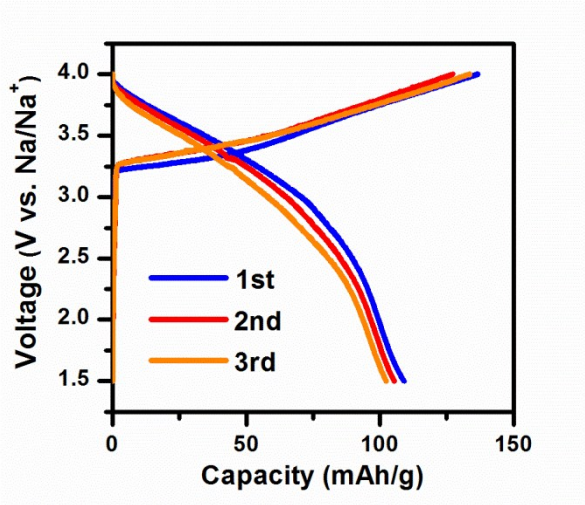

Figure S8 Charge-discharge profiles of $Na_{0.8}Ni_{0.4}Ti_{0.6}O_2$ for the first three cycles.

The excellent full cell performance should be attributed to the high efficiency of both cathode and anode. For the cathode side, the charge-discharge profiles of $Na_{0.8}Ni_{0.4}Ti_{0.6}O_2$ for the first three cycles displayed a low efficiency (about 80 %), which is caused by the decomposition of electrolyte at high charge cut-off voltage. In the full cell, the cut-off voltage is 3.6 V, which could much reduce the inefficiency of the cathode.[17] Thus, the full cell could present an excellent cycling performance.

Reference:

1. K. Shen and M. Wagemaker, *Inorgnic Chemistry*, 2014, **53**, 8250-8256.

2. J. Xu, C. Ma, M. Balasubramanian and Y. S. Meng, *Chemical Communications*, 2014, **50**, 12564-12567.

3. P. J. Naeyaert, M. Avdeev, N. Sharma, H. B. Yahia and C. D. Ling, *Chemistry of Materials*, 2014, **26**, 7067-7072.

4. H. Yu, Y. Ren, D. Xiao, S. Guo, Y. Zhu, Y. Qian, L. Gu and H. Zhou, *Angewandte Chemie*, 2014, **126**, 9109-9115.

5. R. Shanmugam and W. Lai, *ECS Electrochemistry Letters*, 2014, **3**, A23-A25.

6. B. Qu, C. Ma, G. Ji, C. Xu, J. Xu, Y. S. Meng, T. Wang and J. Y. Lee, *Advanced Materials*, 2014, **26**, 3854-3859.

7. S. Yuan, X. l. Huang, D. l. Ma, H. g. Wang, F. z. Meng and X. b. Zhang, *Advanced Materials*, 2014, **26**, 2273-2279.

8. L. David, R. Bhandavat and G. Singh, *ACS Nano*, 2014, **8**, 1759-1770.

9. W. Li, S. L. Chou, J. Z. Wang, J. H. Kim, H. K. Liu and S. X. Dou, *Advanced Materials*, 2014, **26**, 4037-4042.

10. Y. Dong, S. Li, K. Zhao, C. Han, W. Chen, B. Wang, L. Wang, B. Xu, Q. Wei and L. Zhang, *Energy & Environmental Science*, 2015, **8**, 1267-1275.

11. J. Billaud, G. Singh, A. R. Armstrong, E. Gonzalo, V. Roddatis, M. Armand, T. Rojo and P. G. Bruce, *Energy & Environmental Science*, 2014, **7**, 1387-1391.

12. Y. Zhang, L. Guo and S. Yang, *Chemical Communications*, 2014, **50**, 14029-14032.

13. Y. Wang, J. Liu, B. Lee, R. Qiao, Z. Yang, S. Xu, X. Yu, L. Gu, Y.-S. Hu and W. Yang, *Nature Communications*, 2015, **6**.

14. Y. Wang, R. Xiao, Y.-S. Hu, M. Avdeev and L. Chen, *Nature Communications*, 2015, **6**.

15. D. Wu, X. Li, B. Xu, N. Twu, L. Liu and G. Ceder, *Energy & Environmental Science*, 2015, **8**, 195-202.

16. J. Wang, B. Qiu, X. He, T. Risthaus, H. Liu, M. C. Stan, S. Schulze, Y. Xia, Z. Liu and M. Winter, *Chemistry of*

Materials, 2015.

17 S. Guo, H. Yu, P. Liu, Y. Ren, T. Zhang, M. Chen, M. Ishida and H. Zhou, *Energy & Environmental Science*, 2015, **8**, 1237-1244.